Fast visible camera installation and operation in JET

J. A. Alonso[1], P. Andrew[2], A. Neto[3], J. L. de Pablos[1], E. de la Cal[1], H. Fernandes[3], J. Gafert[4], P. Heesterman[2], C. Hidalgo[1], G. Kocsis[5], A. Manzanares[1], A. Murari[6], G. Petravich[5], L. Rios[1], C. Silva[3] and P.D. Thomas[2] and JET EFDA contributors[*]

[1]*Asociación EURATOM-CIEMAT, Av. Complutense 22, 28020 Madrid – Spain*
[2]*EURATOM-UKAEA Association, Culham Science Center, Abingdom – UK*
[3]*Associação EURATOM-IST, Av. Rovisco Pais, 1049-001 Lisbon – Portugal*
[4]*Max-Planck IPP, Boltzmannstrasse 2D-85748 Garching – Germany*
[5]*EURATOM-HAS Association, KFKI-RMKI, P.O.Box 49, H-1525 Budapest-114 - Hungary*
[6]*Consorzio RFX-Associazione EURATOM ENEA per la Fusione, I-35127 Padova – Italy*

This article is a summary of the measurements of the recently installed wide-view fast visible camera in the Joint European Tokamak JET. Here we limit ourselves to a description of the different phenomena and leave for forthcoming articles a more extensive analysis of every phenomenon.

1. Camera system and technical issues

A fast visible Photron APX-RS camera has recently been installed on JET. The camera is located near the equatorial plane of octant 8 and is looking through an endoscope designed for infrared imaging [1]. It uses a CMOS detector with a maximum recording speed of 250 kHz and a minimum exposure time of 1 us. In the present set-up a commercial camera lens and no filters are used. The camera was tested against high radiation fluxes and rapidly varying magnetic fields. The integrated neutron fluence in the camera position after four months of operation is in the range of 4×10^{10} n/cm^2. So far there is no evidence of permanently damaged pixels. Several disruptions were recorded the camera withstanding field variations of up to 4 T/s.

2. Observed phenomena and first estimations

2.1 ELM physics and plasma-wall interaction - The fast camera has proven to provide useful information to study different fusion plasma relevant issues including plasma wall interaction, ELMs and disruption physics. Figure 1 shows the expulsion of macroscopic particles from the wall after the occurrence of an ELM.

---

[*] See Apendix of M.L. Watkins et al., Fusion Energy 2006 (Proc. 21st Int. Conf. Chengdu, 2006, IAEA)

Figure 1. Particle expulsion from a poloidal limiter. Images are taken at 3 kfps with 166 us exposure time.

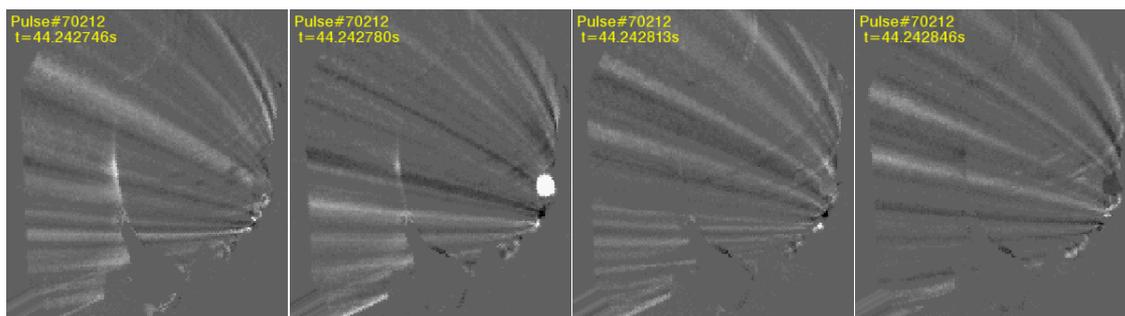*Figure 2. Filament development during an ELM (30 kfps, 25us exp. time). The background images (calculated as the pixel median over 500 us) has been subtracted from the original frames to highlight the filamentary structure.*

Some 6 ms after the sudden radiation increase caused by an ELM, a shower of solid fragments is seen to come out of an outer wall poloidal limiter and seem to be accelerated in the toroidal co-current direction (that is also the direction of the parallel plasma flows for this configuration). These particles can be seen for 50 ms.

ELMs are commonly seen in the images as a sudden increase of radiation. For high power type-I ELMs like the one in figure 2, an associated filamentary structure can be observed as in other machines [2], [3]. In the high frequency recording of an ELM in figure 4, a helical interaction pattern can be seen on the wall within 40 us following the onset of the ELM (the associated D_α rise). This kind of interaction pattern has also been seen with infrared cameras in JET [4]. It should be noted that an ELM impact can produce localized particle desorption from the wall elements. These particles are transported parallel to the magnetic field and can also be seen as filamentary structures (figure 4, third and fourth frames) which are thus different from the ELM own structure.

2.2 ELM radial / parallel dynamics - Very fast framing can be achieved if the active part of the detector is reduced. Images in figure 3, show a 100 kfps frame sequence of the divertor during an ELM. The radiation increase starts very close to the
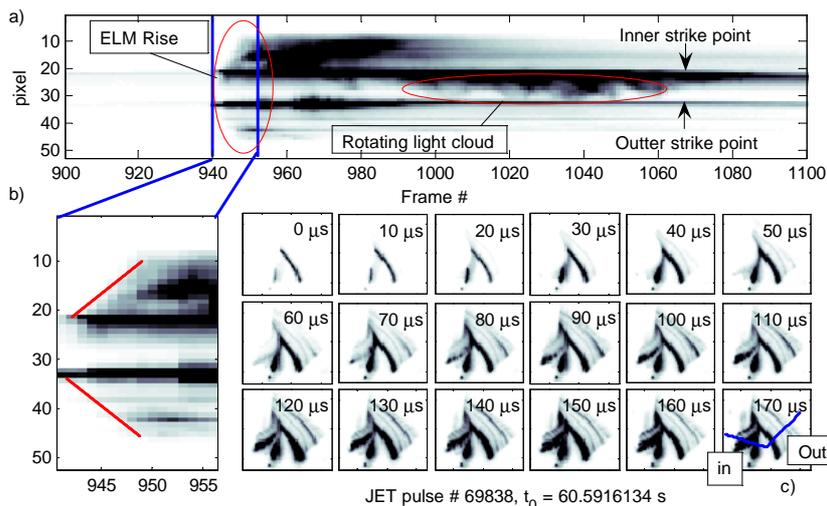
Figure 3. (a) Time trace of the pixels on the blue line in the last frame of (c) -approx. in a poloidal section. The radiation onset shows a delayed arrival to the ELM energy flux to the different divertor positions. (b) Close-up of the ELM rise. (c) Sequence of the divertor at the ELM onset (@ 100 kfps 9 us exposure).

strike points (figure 3). The D_α rise progressively reaches further divertor positions up to the limiters shadows. Two possible causes of this delayed arrival have been identified as the radial decay of the parallel flow because of the SOL temperature profiles [4] and the intrinsic ELM radial velocity. The relative importance of these two factors is under investigation.

From figure 3 it is apparent that the volume light emission from inner divertor is stronger that that of the outer, consistently with the measured higher neutral density. An intensively radiating cloud localized in between the strike points is seen after the impact of some ELMs and appears to rotate in the toroidal direction (figure 3.a).

2.3 Plasma Disruptions - During disruptions (figure 5) the plasma detaches from the divertor as the current is lost and high particle fluxes are directed to the wall. MHD activity can also be seen as fillamentation. In the course of a disruption a highly radiating MARFE-like ring could be seen which travels from the upper plate, where it formed, to the equatorial plane in the HFS in ~5ms, where it keeps radiating for ~32 ms. After this time the plasma terminates violently.

3. Conclusions and future plans

The recently installed fast visible camera in JET has produced the first results. Several physical phenomena like particle expulsion from the wall, ELM filamentation, MARFE formation and disruptions have been observed. The apparent toroidal rotation velocities of the structures during ELMs and disruptions were estimated from the images to be in the order of 10 km/s. ELMs can be seen to reach the first wall less than 40 us after the start of the light rise giving, for a typical wall clearance of 40 mm, radial propagation velocities in the range of 1

km/s. More extensive analysis of the individual phenomena, here only briefly described, will be carried out in future articles. Investigations of the pellet-plasma interaction will also be studied by making use of the camera system capabilities.

The study of lower intensity phenomena, like the continuous plasma wall interaction and the generation and dynamics of impurities, requires a higher signal level. Image intensifiers are being tested for its possible installation on JET fast imaging system, which would allow the use of interference filters so as to investigate these and other phenomena. Image analysis techniques for optical flow estimation, spatial-temporal structure detection and IR/visible data merging are under development [6].

Figure 4. ELM onset and interaction with the wall (@ 30 kfps 25 us exposure). A helical wall-interaction pattern can be seen less than 40 us after the start of the D_α rise.
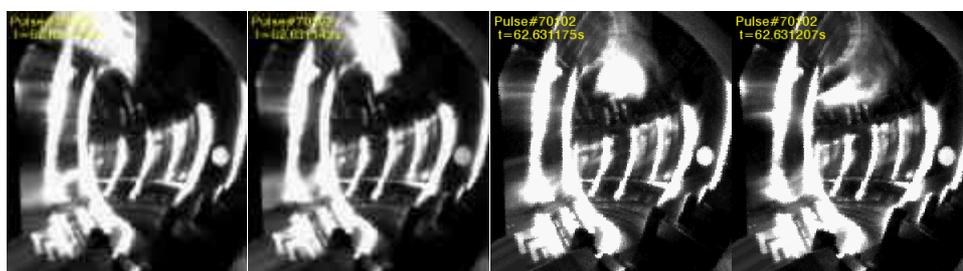

Figure 5. JET interior during a plasma disruption (@ 30 kfps, 25us exp. time). The magnetic configuration is largely lost and the plasma interacts strongly with the inner and outer walls. A light cloud is seen to move toroidally in the counter-current direction . It moves ~90 deg in the toroidal direction in the lapse of 3 frames. For R=3m this gives ~$4x10^4$ m/s

Bibliography

[1] E. Gauthier et al, Proc. of the 17th PSI Conference, Heifei, China 22-26/05/2006

[2] A. Kirk, H. R. Wilson *et al.,* Phys. Rev. Lett. **92**, 245002 (2004)

[3] R. J. Maqueda, R. Maingi, *et al.*, J. Nucl. Mater. 363-365, (2007)

[4] P. Andrew *et al.,* these proceedings.

[5] R. Pitts *et al.*, Nuclear Fusion **46** (2006) 82

[6] S. Hong, A. Murari *et al.,* these proceedings.